Synthesis, physicochemical properties and antioxidant activity of deferiprone–cyclodextrin conjugates and their iron(III) complexes

ARTICLE *in* DALTON TRANSACTIONS · NOVEMBER 2011

Impact Factor: 4.2 · DOI: 10.1039/c1dt11677k · Source: PubMed

Dalton Transactions

An international journal of inorganic chemistry

www.rsc.org/dalton

Volume 41 | Number 10 | 14 March 2012 | Pages 2837–3096

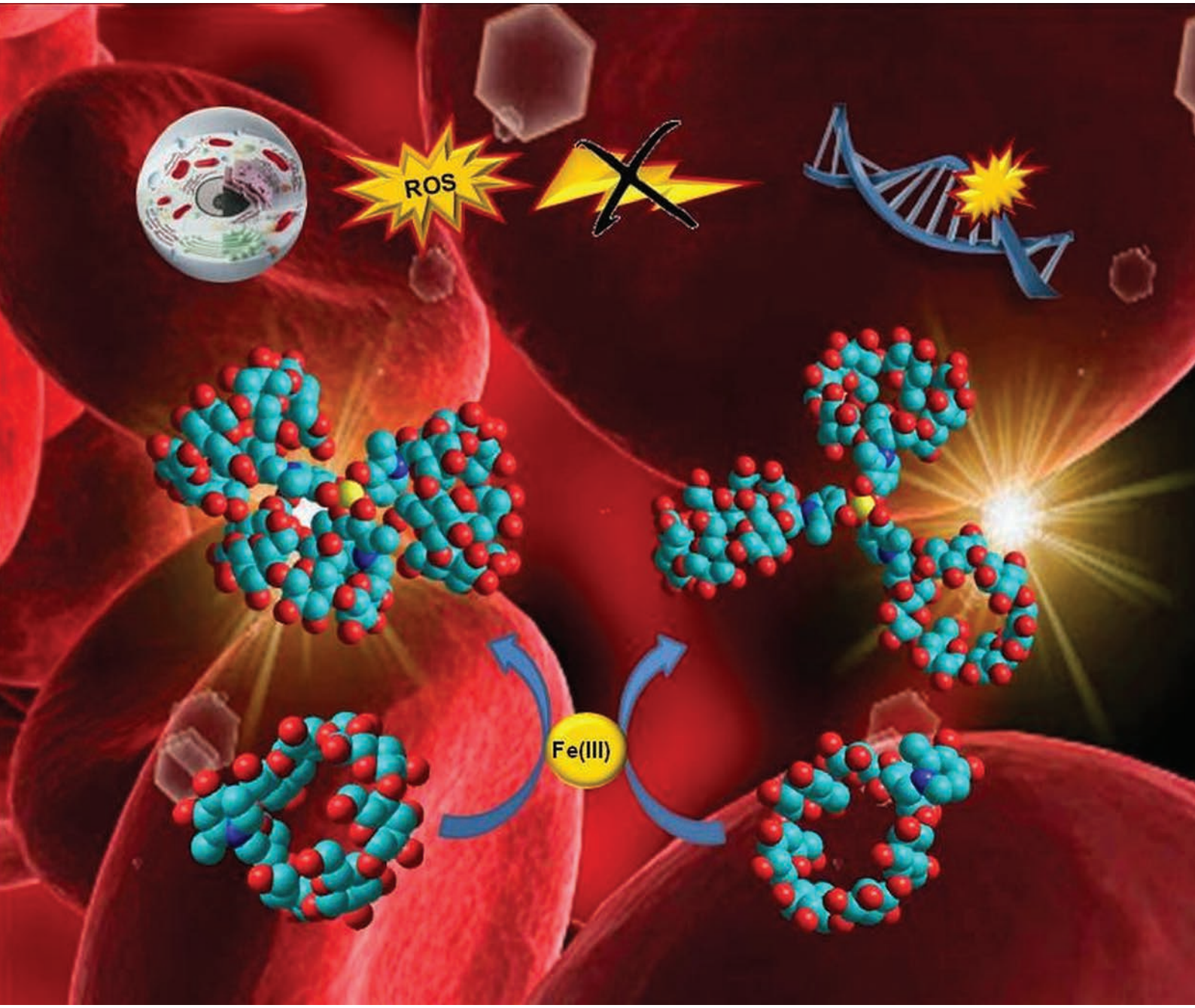

ISSN 1477-9226

RSC Publishing

COVER ARTICLE

Puglisi, Spencer *et al.*

Synthesis, physicochemical properties and antioxidant activity of deferiprone-cyclodextrin conjugates and their iron(III) complexes

1477-9226(2012)41:10;1-X

Dalton Transactions

Dynamic Article Links

Cite this: *Dalton Trans.*, 2012, **41**, 2877

www.rsc.org/dalton

PAPER

Synthesis, physicochemical properties and antioxidant activity of deferiprone-cyclodextrin conjugates and their iron(III) complexes†

Antonino Puglisi,*[a] John Spencer,*[a] Valentina Oliveri,[b] Graziella Vecchio,[b] Xiaole Kong,[c] James Clarke[d] and John Milton[d]

Received 5th September 2011, Accepted 24th October 2011
DOI: 10.1039/c1dt11677k

3-Hydroxy-1,2-dimethylpyridin-4(1*H*)-one (deferiprone) is a successful iron chelator, which has been widely investigated for its activity in mitigating iron overload and in protecting against oxidative stress due to Reactive Oxygen Species (ROS). Herein, we present the synthesis, characterisation, physicochemical properties and antioxidant activity of two novel bioconjugates of β-cyclodextrin bearing the deferiprone moiety either on the upper rim (**1**) or on the lower rim (**2**) of the cyclodextrin and their iron(III) complexes. Protonation and iron stability constants were measured by spectrophotometric titration for the two systems and antioxidant activity studied for both the ligands and the iron(III) complexes.

Introduction

Iron plays a fundamental role in numerous essential metabolic processes. Its homeostasis is maintained through a sophisticated regulatory mechanism of uptake, storage and secretion. Excessive or misplaced tissue iron now is recognised to pose a substantial risk for endocrinological, gastrointestinal, infectious, neoplastic, neurodegenerative, obstetric, ophthalmic, orthopaedic, pulmonary and vascular diseases.[1] The two most common and serious forms of iron overload result from genetic cause (haemochromatosis) and transfusional iron overload.[2] The latter is a side effect of life-sustaining blood transfusions for the treatment of disorders such as β-thalassemia and sickle cell anaemia. Iron chelators are used in medicine to protect patients from the consequences of iron overload and iron toxicity. Hydroxypyridinones are a successful class of iron chelators.[3] Some noteworthy molecules containing the 3-hydroxy-4-piridinone framework possess also antineoplastic[4] and anti-inflammatory[5] activity. 3-Hydroxy-1,2-dimethylpyridin-4(1*H*)-one, known as deferiprone (Fig. 1), in particular, exhibits high stability constants with iron (III) and, in some countries in Europe, is in clinical use as an oral chelator to mitigate iron overload in thalassemia[6] and multiple transfusion patients. Deferiprone (HPO) possesses also antioxidant properties protecting against oxidative stress due to Reactive Oxygen Species (ROS) and recently its use has been reported for potential application in the treatment of neurodegenerative diseases[7] such as Alzheimer's.[8] The basic structure of HPO can be functionalised either by *N*- or *O*-substituent variation. *N*-substituents, in particular, are very interesting as they can alter the physico-chemical properties of the drug without significantly changing the metal iron binding capacity.[9]

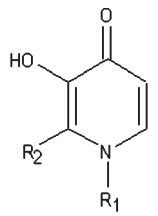

Fig. 1 3-Hydroxy-4-pyridinone basic structure.

Recently, carbohydrate-bearing deferiprones have been investigated by various groups to impart elevated brain uptake,[10,11] or with radioactive elements for applications in diagnostic nuclear medicine.[12]

The excellent qualities of HPO as a low toxicity metal chelator and antioxidant inspired us to functionalise it with the oligosaccharidic structure of a β-cyclodextrin (β-CD).

The conjugation with the β-CD moiety might impart some specific characteristics to the resulting molecules: a) improve the pharmacokinetics of the drug by preventing metabolism and excretion (*e.g.* glucuronidation),[13] b) potentially increase aqueous solubility,[14,15] c) provide a hydrophobic cavity which can enable the conjugates to form inclusion complexes with co-formulating drugs, d) potentially deliver specifically the HPO to the colon.[16,17]

[a]*School of Science, University of Greenwich at Medway, Chatham, Kent, ME4 4TB, UK. E-mail: a.puglisi@greenwich.ac.uk, j.spencer@greenwich.ac.uk; Fax: 44(0)208 331 9805; Tel: 44(0)208 331 8215*
[b]*Department of Chemistry, University of Catania, V.le A. Doria 6, 95125, Italy*
[c]*Institute of Pharmaceutical Science, King's College London, Franklin-Wilkins Building, 150 Stamford Street, London, SE1 9NH, UK*
[d]*Oxford Nanopore Technologies Ltd., Edmund Cartwright House, 4 Robert Robinson Avenue, Oxford Science Park, Oxford, OX4 4GA, UK*
† Electronic supplementary information (ESI) available: NMR and ESI-MS spectra of ligands and speciation plots. See DOI: 10.1039/c1dt11677k

Herein, we report the synthesis, characterisation, physico-chemical properties and antioxidant activity of two novel β-CD conjugates with the HPO moiety covalently linked either on the upper rim **1** (position 6) or on the lower rim **2** (position 3) of the β-CD (Fig. 2).

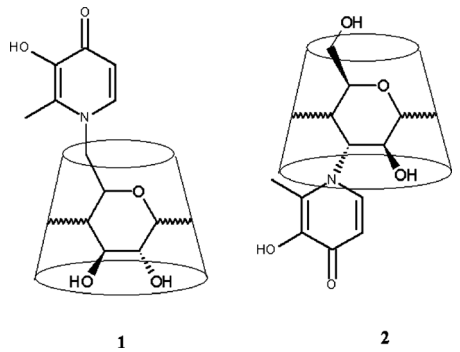

Fig. 2 Schematic representation of the deferiprone-cyclodextrin conjugates **1** and **2**.

Experimental

Synthesis

The two deferiprone-cyclodextrin conjugates were synthesised from the corresponding mono-amino-cyclodextrins in position 6 and 3 according to Scheme 1.

***6A-deoxy-6A-N-(2-methyl-3-hydroxypyridin-4-one)-β-cyclodextrin* (1).** 6A-deoxy-6A-amino-β-cyclodextrin[18] (150 mg, 0.132 mmol) was dissolved in H_2O/MeOH (2 ml/2 ml) together with 3-(benzyloxy)-2-methyl-*4H*-pyran-4-one (60 µl, 0.327 mmol; *ca* 2.5 : 1) and NaOH (50 µl, 3.8 M). The mixture was stirred and heated at 75 °C overnight. The cooled mixture was evaporated to dryness and the benzylated intermediate isolated by HPLC (SunFire PrepC18 5 µm 10 × 150 mm - MeOH/Water (30 : 70) - 1 ml min^{-1}) and characterised by ESI-MS. Debenzylation of the intermediate was performed by catalytic hydrogenolysis. The isolated benzylated intermediate was dissolved in H_2O/MeOH (8 ml/8 ml) and *ca* 20 mg of Pd/C (10% w/w) were added. The suspension was stirred at room temperature overnight under an atmosphere of H_2. After filtration, the solution was brought to dryness, dissolved in a minimum amount of water and precipitated in *ca* 100 ml of acetone and the resulting solid was collected by filtration and air dried. The yield (*ca* 80%) was calculated on the isolated final products.

Rf (2PrOH:AcOEt:H_2O:NH_3/5 : 2 : 3 : 3) = 0.14.

ESI-MS (*m*/*z*) 1242.5 (M+1).

HRMS-ES (*m*/*z*) found 1242.4142; calcd for $[C_{48}H_{75}NO_{36}+H]^+$ 1242.4142.

^{1}H NMR (500 MHz, D_2O): 7.20 (s, 1H, H-*ortho*-HPO ring), 6.28 (s, 1H, H-*meta*-HPO ring), 5.10–4.80 (m, 7H, H1), 4.52 (d, 1H, H6A),4.15–3.25 (m, 39H, H2, H3, H4, H5, H6′A, H6C-G), 3.02 (d, 1H, H6B), 2.76 (d, 1H, H6′B), 2.28 (s, 3H, -CH_3 HPO ring).

^{13}C NMR (100 MHz, D_2O): 169.8 (C═O); 146.0 (CH *ortho* HPO ring); 134.6 (CH–OH HPO ring); 128.5 (CH–CH_3 HPO ring); 112.3 (CH *meta* HPO ring); 102.0 (C-1); 81.3 (C-4); 73.3 (C-2); 72.1 (C-5); 71.9 (C-3); 60.3 (C-6); 55.0 (C-6A); 12.1 (CH_3 HPO ring).

***3A-N(2-methyl-3-hydroxypyridin-4-one)-3A-deoxy-2A(S),3A(R)-β-cyclodextrin* (2).** **2** was synthesised similarly to **1** from 3A-amino-3A-deoxy-2A(S),3A(R)-β-cyclodextrin (purchased and used as such from TCI, Tokyo Chemical Industry Co., Ltd).

Rf (2PrOH:AcOEt:H_2O:NH_3/5 : 2 : 3 : 3) = 0.16.

ESI-MS (*m*/*z*) 1242.9 (M+1); 622.2 (M+2)/2.

HRMS-ES (*m*/*z*) found 1242.4128; calcd for $[C_{48}H_{75}NO_{36}+H]^+$ 1242.4142.

^{1}H NMR (500 MHz, D_2O): 7.83 (s, 1H, H-*ortho*-HPO ring), 6.46 (s, 1H, H-*meta*-HPO ring), 5.15–4.85 (m, 7H, H1), 4.31 (m, 1H, H2A), 4.06 (m, 1H, H4A), 3.95–3.39 (m, 39H, H2C-G, H3, H4B-G, H5, H6), 3.34 (d, 1H, H2B), 2.35 (s, 3H, -CH3).

^{13}C NMR (100 MHz, D_2O): 171.1 (C═O); 152.0 (CH HPO ring); 135.3 (CH–OH HPO ring); 128.0 (CH–CH_3 HPO ring); 112.7 (CH HPO ring); 104.0–101.5 (C-1); 81.0 (C-4); 77.0 (C-4A); 76.5 (C-5A); 73.3 (C-2); 72.1 (C-5); 71.9 (C-3); 70.6 (C-2B); 67.3 (C-2A); 60.3 (C-6); 12.0 (CH_3 HPO ring).

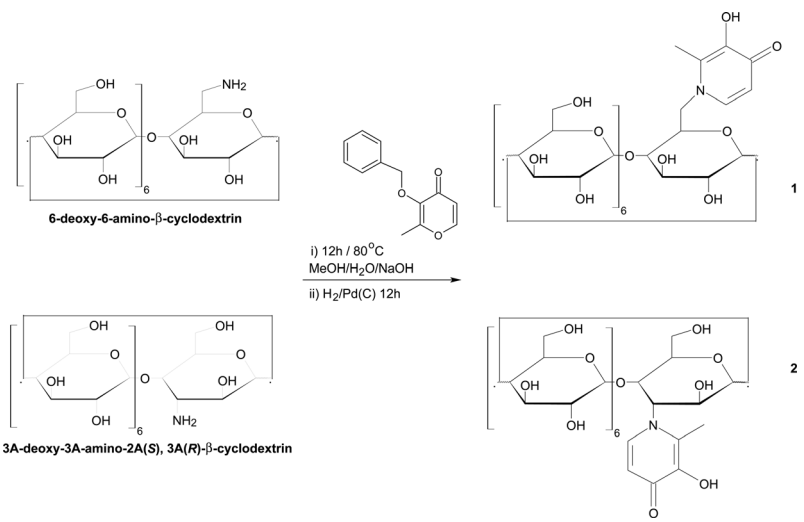

Scheme 1 Synthesis of **1** and **2**.

pK_a and iron stability constants

The automatic titration system used in this study comprised an autoburette (Metrohm Dosimat 765 litre ml syringe) and Mettler Toledo MP230 pH meter with Metrohm pH electrode (6.0133.100) and a reference electrode (6.0733.100). 0.1 M KCl electrolyte solution was used to maintain the ionic strength. The temperature of the test solutions was maintained in a thermostatic jacketed titration vessel at 25 °C ± 0.1 °C by using a Techne TE-8J temperature controller. The solution under investigation was stirred vigorously during the experiment. A Gilson Miniplus#3 pump with speed capability (20 ml min^{-1}) was used to circulate the test solution through a Hellem quartz flow cuvette. For the stability constant determinations, a 50 mm path length cuvette was used, and for pK_a determinations, a cuvette path length of 10 mm was used. The flow cuvette was mounted on an HP 8453 UV-visible spectrophotometer. All instruments were interfaced to a computer and controlled by a Visual Basic program. Automatic titration and spectral scans adopted the following strategy: the pH of a solution was increased by 0.1 pH unit by the addition of KOH from the autoburette; when pH readings varied by <0.001 pH unit over a 3 s period, an incubation period was activated. For pK_a determinations, a period of 1 min was adopted; for stability constant determinations, a period of 5 min was adopted. At the end of the equilibrium period, the spectrum of the solution was then recorded. The cycle was repeated automatically until the defined end point pH value was achieved. All the titration data were analysed with the pHab program.[19] The species plot was calculated with the HYSS program.[20] Analytical grade reagent materials were used in the preparation of all solutions.

NMR spectroscopy

NMR spectra were recorded at 25 °C in D_2O with a Varian UNITY PLUS 500 spectrometer. ^{1}H NMR spectra were recorded at 25 °C in D_2O with a Varian UNITY PLUS spectrometer at 499.883 MHz. The ^{1}H NMR spectra were obtained by using a standard pulse programs from the Varian library. In all cases the length of 90° pulse was 7 ms. The 2D experiments were acquired using 1 K data points, 256 increments and a relaxation delay of 1.2 s. T-ROESY spectra were obtained using a 300 ms spin-lock time. DSS was used as external standard.

UV/Visible and circular dichroism spectroscopy

UV/Visible spectra were recorded with an Agilent 8452A diode array spectrophotometer. All measurements were carried out at 25 ± 0.2 °C using 1 × 1 cm thermostated cuvettes in which solutions were magnetically stirred. Circular dichroism measurements were performed under a constant flow of nitrogen on a JASCO model J-810 spectropolarimeter. The spectra represent the average of 5 scans and were recorded at 25 °C, on freshly prepared aqueous solutions.

Superoxide Dismutase (SOD) assay

SOD-like activity was determined by the indirect method of Nitro Blue Tetrazolium (NBT) reduction.[21] Superoxide radical anion was enzymatically generated by the xanthine-xanthine oxidase (XO/XOD) system and spectrophotometrically detected by monitoring the formation of reduced NBT at 550 nm. The reaction mixture was composed of NBT 250 μM, xanthine 50 μM, catalase 30 μg ml^{-1} in phosphate buffer 10 mM, at pH 7.4. An appropriate amount of xanthine oxidase was added to 2.0 ml reaction mixture to produce a $\Delta A_{550\ nm}$ min^{-1} of 0.024. This corresponded to a $O_2^{\cdot -}$ production rate of 1.1 μmol min^{-1}. The NBT reduction rate was measured in the presence and in the absence of the investigated complex for 600 s. Stock solutions of complexes were prepared by mixing an acid solution of $FeCl_3$ and ligand with a ratio 1 : 3 in phosphate buffer 10 mM, pH 7.4. In separate experiments urate production by xanthine oxidase was spectrophotometrically monitored at 295 nm, ruling out any inhibition of xanthine oxidase activity. The I_{50} (the concentration which causes the 50% inhibition of NBT reduction) of iron(III) complexes at pH 7.4 was determined. Three determinations were carried out in order to generate consistent data with statistical errors.

Trolox Equivalent Antioxidant Capacity (TEAC) assay

The antioxidant capacity of the β-CD derivatives was determined by the 2,2′-azinobis-(3-ethylbenzothiazoline-6-sulphonic acid diammonium salt (ABTS) radical cation decolourisation assay[22] using 6-hydroxy-2,5,7,8-tetramethylchroman-2-carboxylic acid (Trolox) as a standard. In brief, the radical cation $ABTS^{+\cdot}$ was generated by a reaction between ABTS (7 mM) and persulphate (2.45 mM) in water. After a 16 h incubation (dark, room temperature) the resulting solution was diluted in a cuvette with phosphate buffer (10 mM, pH 7.4) such that the absorbance of the solution at 734 nm was 0.7 ± 0.02. This radical solution was combined with sample antioxidants, in varying concentrations, and allowed to react for six minutes. All samples were diluted approximately to provide 20–80% inhibition of the blank absorbance. The absorbance values were measured for 6 min. Solution absorbance was plotted *vs.* test compound concentration; each resultant slope was normalised with respect to that obtained for Trolox to give the Trolox-equivalence (TEAC) value for each time point (1, 3, 6 min). All determinations were carried out at least three times and in triplicate at each separate concentration of the samples in order to generate consistent data with statistical errors.

Results and discussion

Synthesis of the ligands

We set out to synthesise the two systems functionalised in position 6 and in position 3 of the β-CD in order to compare the role played by the two different rims of the hydroxyl groups of the β-CD on the HPO chelating and antioxidant activities. Derivatives in position 3 have in fact been shown to have different physicochemical properties compared to their position 6 analogues.[23]

1 and **2** were synthesised similarly from the corresponding mono-amino-β-CD compounds in position 6 and in position 3 by reaction with 3-(benzyloxy)-2-methyl-4*H*-pyran-4-one (benzyl maltol) and subsequent debenzylation.

NMR

NMR spectra confirm the identity of the ligands. In the ^{1}H NMR spectrum of **1**, the H-6A diastereotopic protons are evident at

4.52 and 4.03 ppm. These protons are significantly shifted downfield due to the aromatic moiety. In the spectra the H-6B protons appear at 3.01 and 2.75 ppm and are shifted upfield due to the ring effect of the HPO moiety as previously reported for aromatic moieties directly bound to the H-6.[24] The ^{1}H NMR spectrum of **2** shows together with the signals due to the β-CD protons at 4.0–3.4 ppm, the signals due to the functionalised A ring. As a consequence of the 3-functionalisation, signals due to the H-3A and H-5A appear at 4.75 and 4.30 ppm, significantly shifted downfield for the aromatic functionalising moiety. All the other protons of A ring are easily identified by COSY spectra. The B ring is significantly influenced by the ring effect of the HPO and the 2B proton can be identified at 3.37 ppm. The signals due to the protons of the HPO moiety appear at aromatic region and at 2.39 ppm. The coupling constant values between H-1A and H-2A ($J_{1A,2A}$ = 6.6 Hz) and between H-2A and H-3A ($J_{2A,3A}$ = 11.0 Hz) indicate that 1A, 2A, 3A protons are axial. These values are in keeping with the predominately $^1C_4$ conformation reported for this class of derivatives.[25–27]

The ROESY spectra of the conjugates do not show any correlation between the cavity and the HPO unit for compound **1**, while for compound **2** a correlation is evident between protons H-6 and H-3 of the functionalised ring thereby suggesting an interaction of the HPO moiety with the cavity. The HPO residue is presumably not completely self-included into the β-CD cavity due to shortness of the chain.

Circular dichroism

The ligands were characterised by circular dichroism spectra, in order to further investigate the interaction of HPO ring with the β-CD cavity. The circular dichroism spectrum of **2** shows two intense negative bands in the UV region. The band centred at 280 nm is due to the dipole–dipole coupling between the HPO moiety and the β-CD cavity. This behaviour has been generally reported for functionalised CDs and is due either to the inclusion of the functionalising moiety in the cavity or its proximity. In this case deep inclusion of the side chain cannot be proposed on the basis of NMR spectra and so the proximity of the side chain to the lower rim could be hypothesised. The orientation of the pendant included into the β-CD cavity can be deduced using the rules for Induced Circular Dichroism (ICD). The sign is positive for a transition polarised parallel to the axis of the macrocyclic and negative for that perpendicular to the axis. The rule is reversed for a chromophore that moves from the inside to outside, keeping the direction of the transition moment uncharged.[28,29] The spectrum is affected by the presence of 1-adamantanol (ADM), a competitive guest of β-CD cavity. The reduction in intensity of the dichroic bands with increasing concentration of ADM reveals a slight displacement of the HPO moiety from the β-CD cavity. Even when a large excess of ADM was added the circular dichroism signal is maintained (Fig. 3). ADM is in fact included into the β-CD cavity through the secondary rim[30] in keeping with the displacement of HPO outside the β-CD cavity. In the case of **1**, the circular dichroism spectra show only a very weak band, in keeping with the proximity of the aromatic ring to the cavity. No significant changes were observed when ADM was added, in keeping with the orientation outside the cavity of the HPO moiety.

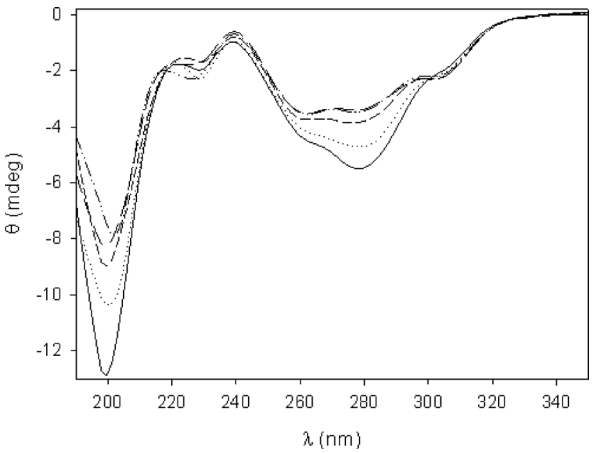

Fig. 3 Circular dichroism spectra of **2** (1.2×10^{-3} M) alone (solid line) and in the presence of increasing amounts of ADM (1.2×10^{-3} M–1.2×10^{-2} M).

Table 1 pK_a values for HPO and the two conjugates (0.1 M KCl at 25 °C)

	HPO	1	2
pK_{a1}	3.663 (*1*)	2.983 (*6*)	3.052 (*2*)
pK_{a2}	9.756 (*1*)	9.602 (*2*)	9.630 (*1*)

Values in parentheses are standard deviations on the last significant figure.

Proton and iron complex stability constants

The 3-hydroxy-4-pyridinone framework of the HPO moiety possesses two protonation equilibria. Ka_1 is associated with the protonation of the 4-oxo-group and Ka_2 with the protonation of the 3-hydroxyl group (Fig. 4). For the protonation on the carbonyl oxygen has been clearly demonstrated[31] the involvement of two H_2L species, respectively, on nitrogen and carbonylic oxygen. In comparison with HPO,[32] both compounds **1** and **2** have lower pK_{a1} values by approximately 0.5 units (Table 1) which can be attributed to the effect of the CD. In fact, a decrease in the values of the protonation constant for the amino group bound to C-6 or C-3 of the functionalised glucose ring has been reported in the literature for a number of CD derivatives studied by potentiometry.[33] This behaviour has been attributed to hydrogen bonding as well as to the steric and hydrophobic effects of the CD cavity. The effect is rather small in keeping with the only

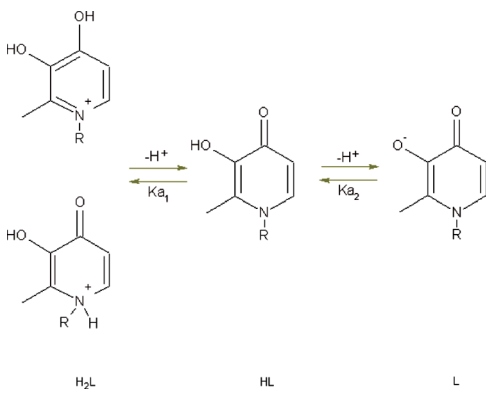

Fig. 4 Protonation equilibria for deferiprone derivatives.

Table 2 Iron(III) stability constants for HPO and the two conjugates (0.1 M KCl at 25 °C)

	HPO	1	2
$\log\beta_1$	15.086 (*2*)	15.023 (*2*)	14.994 (*3*)
$\log\beta_2$	27.357 (*3*)	27.070 (*2*)	27.086 (*3*)
$\log\beta_3$	37.089 (*3*)	37.049 (*2*)	37.105 (*4*)

Values in parentheses are standard deviations on the last significant figure.

partial involvement of the amino group in the protonation equilibria. Moreover a slight decrease of the pK_{a1} has also been observed for the *N*-alkylation of HPO.[34]

The β-CD derivatives **1** and **2** are able to complex iron(III) with the same stability as HPO (Table 2). The iron(III) complex species are formed with the 3-hydroxyl group of deferiprone deprotonated (L in the speciation plot). Despite the large dimension of the β-CD unit of the conjugates the iron(III) complexes do not appear to display any steric hindrance towards the formation of 3 : 1 iron(III) complexes. Molecular models (*Hyperchem 8.0*) of iron complexes of **1** and **2** are shown in Fig. 6 and 7. The iron(III) chelating ability for the two conjugates is the same as the HPO function in keeping with the fact that the chelating oxygens are distant enough from the CD cavity unlike in other CD derivatives.[35] Speciation plots for the two iron(III) complexes are reported in Fig. 5 and in the Electronic Supplementary Information.† The FeL_3 species dominate over the pH 6.5–10 range.

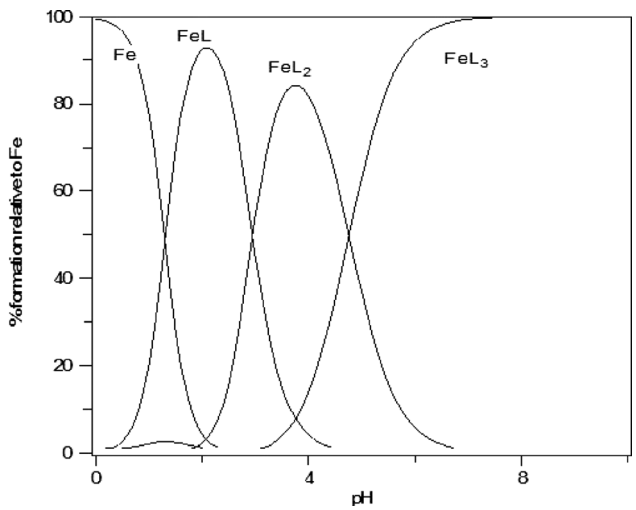

Fig. 5 Speciation plot of **1** (L). 10 μM with 1 μM iron(III).

SOD-like activity

Iron induced oxidative damage is believed to be one of the major causes of complications in various forms of iron overload diseases. This renders necessary in many cases chelation therapy based on the use of appropriate iron chelators, such as HPO. Recently the pro-oxidant effect of non-transferrin bound iron complexes has been reviewed.[36] In this context the SOD-like activity of the iron(III) complexes of HPO, could be important in the reduction of side effects due to iron overload in addition to the chelation activity. The SOD activity of iron(III) complexes of

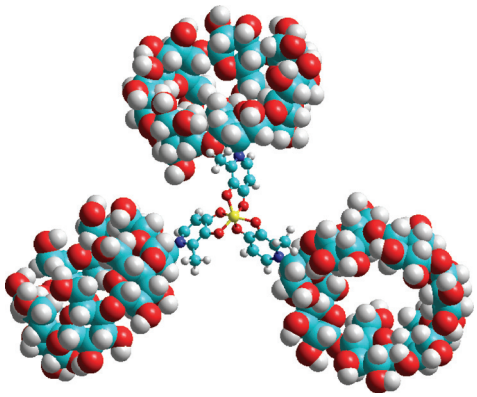

Fig. 6 3D molecular structure of iron complex of **2** (*Hyperchem 8.0*).

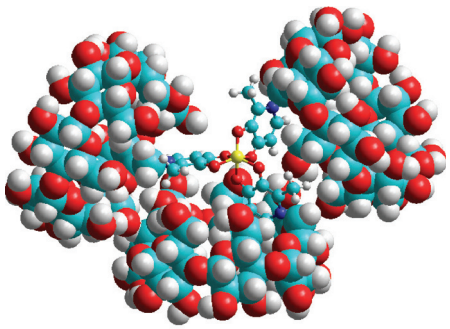

Fig. 7 3D molecular structure of iron complex of **1** (*Hyperchem 8.0*).

Table 3 I_{50} and k_{cat} values of iron complexes FeL_3

L	I_{50} (μM)	k_{cat} (M^{-1} s^{-1})
HPO	16.7 (*9*)	9.4 (*5*) × 10^5
1	6.8 (*5*)	2.2 (*2*) × 10^6
2	15.8 (*8*)	9.3 (*4*) × 10^5

Values in parentheses are standard deviations on the last significant figure.

HPO and β-CD conjugates were determined by competition kinetics using NBT target as reported elsewhere.[37]

Inhibition of target reduction by the complex, when plotted as $V_0/V_{complex}$-1 against the [complex] yielded a straight line. V_0 is the uninhibited reduction rate of NBT by $O_2^{\cdot -}$ and V_{cat} is the rate of reduction of NBT inhibited by the complex. When [complex] is equal to I_{50}, k_{cat}[complex] = $k_{detector}$[detector] and k_{cat} can be determined. $k_{detector}$ is the constant for the reaction between the $O_2^{\cdot -}$ and the detector molecule and it is 5.88 × 10^4 M^{-1} s^{-1} when detector is NBT. The I_{50} values are reported in Table 3. The iron(III) complex of HPO shows a value of I_{50} similar to that reported for this class of compounds.[38] The I_{50} of **2** is the same as that shown by HPO. Interestingly, compound **1** shows a higher activity, the I_{50} is about twice that shown by **2** and HPO. It has been reported for other β-CD conjugates that the proximity of the cavity to the catalytic centre significantly improves the SOD-activity.[39,40] In the HPO conjugates the catalytic moiety is too far away from the cavity to show a large improvement in activity. Furthermore, in the case of **2** the HPO moiety is more rigid and the rim is wider thus no effect of the cavity is shown. This behaviour has been also observed in the

Table 4 TEAC values at 1, 3 and 6 min for tested compounds

	TEAC	TEAC	TEAC
	1 min	3 min	6 min
HPO	1.1 (*1*)	1.3 (*2*)	1.5 (*2*)
1	0.69 (*8*)	0.8 (*1*)	0.9 (*1*)
2	0.50 (*7*)	0.6 (*1*)	0.7 (*1*)

Values in parentheses are standard deviations on the last significant figure.

case of a Mn(III) complex of salophen conjugate with β-CD because of the rigidity and the distance of the catalytic moiety from the cavity. However, in the case of **1**, a significant increase in the SOD activity was found.

Antioxidant capacity of the ligands

Oxidative stress is implicated in a wide variety of processes, diseases and syndromes as outlined earlier. Redox cycling of metal ions can produce reactive oxygen species (ROS) such as the extremely reactive hydroxyl radical, $HO^{\cdot}$, that can abstract hydrogen atoms thereby causing oxidative damage to lipids, proteins, DNA, *etc*. Thus, the ability of drugs to quench radical species in these pathologies is desirable. Hydroxypyridinone derivatives are able to donate hydrogen atoms in a similar manner to that of α-tocopherol (vitamin E) to quench free radicals, and this ability was quantified by the ABTS radical assay. This assay compares the capacity of the test compounds to quench the $ABTS^{+\cdot}$ radical cation in respect to Trolox as reference antioxidant. TEAC values at 1, 3 and 6 min for tested compounds are reported in Table 4. Conjugates **1** and **2** show a slightly lower antioxidant capacity than that of the simple HPO. This behaviour can be explained by the partial inclusion of the HPO moiety in the β-CD cavity. In this case the hydroxyl group of the HPO could be less available to react with radical species. This hypothesis is supported by circular dichroism and NMR data.

Conclusion

In this paper two new deferiprone-β-cyclodextrin conjugates and their iron(III) complexes are reported. Protonation constants and iron(III) chelating ability were investigated for both systems. Antioxidant activity both for the ligands and the iron(III) complexes were studied in comparison with free HPO. We found higher value for SOD activity for the derivative in position 6. This result is in line with what was reported for similar antioxidant systems in which the β-CD seems to play a synergic role in the catalytic process. Furthermore we found that the derivative in position 3 gives rise to a partial phenomenon of self-inclusion of the HPO unit into the β-CD cavity. Apart from potentially improving aqueous solubility due to the presence of the saccharidic residue of the β-CD, the hybrid systems might have interesting characteristics including colon drug delivery and the possibility to form inclusion complexes in the β-CD cavity with coformulating drugs. Moreover the presence of the bulky β-CD moiety might provide a platform for improved pharmacokinetics of the drug conjugates.

Acknowledgements

This work was supported by Oxford Nanopore Technologies Ltd and by MIUR (2008R23Z7K, Firb2011_RBAP114AMK). The EPSRC Mass Spectrometry Unit (Swansea University) is thanked for providing HRMS data. Arunkumar Sarvasuddi is thanked for providing laboratory assistance in this project.

Notes and references

1 E. D. Weinberg, *Metallomics*, 2010, **2**, 732–740.
2 G. J. Kontoghiorghes, E. Eracleous, C. Economides and A. Kolnagou, *Curr. Med. Chem.*, 2005, **12**, 2663–2681.
3 G. J. Kontoghiorghes, M. A. Aldouri, L. Sheppard and A. V. Hoffbrand, *Lancet*, 1987, **1**, 1294–1295.
4 F. Timeus, P. Valle, N. Crescenzio, L. Ruggieri, P. Rosso, G. Luca Pagliardi, L. Cordero di Montezemolo, V. Gabutti and U. Ramenghi, *Am. J. Hematol.*, 1994, **47**, 183–188.
5 G. Ozturk, D. D. Erol, M. D. Aytemir and T. Uzbay, *Eur. J. Med. Chem.*, 2002, **37**, 829–834.
6 R. Galanello, *Ther. Clin. Risk Manag.*, 2007, **3**, 795–805.
7 R. C. Hider, S. Roy, Y. Min Ma, X. Le Kong and J. Preston, *Metallomics*, 2011, **3**, 239–249.
8 L. E. Scott and C. Orvig, *Chem. Rev.*, 2009, **109**, 4885–4910.
9 P. S. Dobbin, R. C. Hider, A. D. Hall, P. D. Taylor, P. Sarpong, J. B. Porter, G. Xiao and D. von der Helm, *J. Med. Chem.*, 1993, **36**, 2448–2458.
10 C. Fernandez, O. Nieto, J. A. Fontenla, E. Rivas, M. L. de Ceballos and A. Fernandez-Mayoralas, *Org. Biomol. Chem.*, 2003, **1**, 767–771.
11 T. P. A. Kruck and T. E. Burrow, *J. Inorg. Biochem.*, 2002, **88**, 19–24.
12 D. E. Green, Cara L. Ferreira, Robert V. Stick, Brian O. Patrick, Michael J. Adam and Chris Orvig, *Bioconjugate Chem.*, 2005, **16**, 1597–1609.
13 H. Schugar, D. E. Green, M. L. Bowen, L. E. Scott, T. Storr, K. Bohmerle, F. Thomas, D. D. Allen, P. R. Lockman, M. Merkel, B. O. Patrick, K. H. Thompson and C. Orvig, *Angew. Chem., Int. Ed.*, 2007, **46**, 1716–1718.
14 B. Gyurcsik and L. Nagy, *Coord. Chem. Rev.*, 2000, **203**, 81–149.
15 D. Bebbington, C. E. Dawson, S. Gaur and J. Spencer, *Bioorg. Med. Chem. Lett.*, 2002, **12**, 3297–3300.
16 K. Minami, F. Hirayama and K. Uekama, *J. Pharm. Sci.*, 1998, **87**, 715–720.
17 K. Uekama, K. Minami and F. Hirayama, *J. Med. Chem.*, 1997, **40**, 2755–2761.
18 A. Puglisi, J. Spencer, J. Clarke and J. Milton, *J. Inclusion Phenom. Macrocyclic Chem.*, 2011, DOI: 10.1007/s10847-011-0054-z, *in press*.
19 P. Gans, A. Sabatini and A. Vacca, *Ann. Chim.*, 1999, **89**, 45–49.
20 L. Alderighi, P. Gans, A. Ienco, D. Peters, A. Sabatini and A. Vacca, *Coord. Chem. Rev.*, 1999, **184**, 311–318.
21 C. Beauchamp and I. Fridovich, *Anal. Biochem.*, 1971, **44**, 276–287.
22 R. Re, N. Pellegrini, A. Proteggente, A. Pannala, M. Yang and C. Rice-Evans, *Free Radical Biol. Med.*, 1999, **26**, 1231–1237.
23 V. Cucinotta, A. Giuffrida, G. Maccarrone, M. Messina, A. Puglisi, E. Rizzarelli and G. Vecchio, *Dalton Trans.*, 2005, 2731–2736.
24 V. Cucinotta, F. D'Alessandro, G. Impellizzeri and G. Vecchio, *J. Chem. Soc., Chem. Commun.*, 1992, 1743–1745.
25 Y. Nogami, K. Nasu, T. Koga, K. Ohta, K. Fujita, S. Immel, H. J. Lindner, G. E. Schmitt and F. W. Lichtenthaler, *Angew. Chem., Int. Ed. Engl.*, 1997, **36**, 1899–1902.
26 D. Q. Yuan, K. Otha and K. Fujita, *J. Chem,. Soc. Chem. Commun.*, 1996, 821–822.
27 K. Fujita, W-H. Chen, D-Q. Yuan, Y. Nogami, T. Koga, T. Fujioka, K. Mihashi, S. Immel and F. W. Lichtenthaler, *Tetrahedron: Asymmetry*, 1999, **10**, 1689–1696.
28 K. Harata, *J. Phys Chem*, 1981, **95**, 2110–2112.
29 B. Balan, D. L. Sivadas and K. R. Gopidas, *Org. Lett.*, 2007, **9**, 2709–2712.
30 R. Breslow, M. F. Czamiecki, J. Emert and H. Hamaguchi, *J. Am. Chem. Soc.*, 1980, **102**, 762–770.
31 V. M. Nurchi, G. Crisponi, T. Pivetta, M. Donatoni and M. Remelli, *J. Inorg. Biochem.*, 2008, **102**, 684–692.
32 R. Hider, P. Taylor, M. Walkinshaw, J. L. Wang and D. Van der Helm, *J. Chem. Res. (S)*, 1990, 316–317.

33 F. Bellia, D. La Mendola, C. Pedone, E. Rizzarelli, M. Saviano and G. Vecchio, *Chem. Soc. Rev.*, 2009, **38**, 2756–2781.
34 B. L. Rai, L. S. Dekhordì, H. Hhodr, Y. Jin, Z. Liu and R. C. Hider, *J. Med. Chem.*, 1998, **41**, 3347–3359.
35 G. I. Grasso, F. Bellia, G. Arena, G. Vecchio and E. Rizzarelli, *Inorg. Chem.*, 2011, **50**, 4917–4924.
36 T. Jirasomprasert, N. P. Morales, L. M. G. Limenta, S. Sirijaroonwong, P. Yamanont, P. Wilairat, S. Fucharoen and U Chantharaksri, *Free Radical Res.*, 2009, **43**, 485–491.
37 I. Spasojevc, I. Batinic-Haberle, D. R. Stevens, P. Hambright, N. A. Thorpe, J. Grodkowski, P. Neta and I. Fridovich, *Inorg. Chem.*, 2001, **40**, 726–739.
38 M. Y. Moridani and P. J. O'Brien, *Biochem. Pharmacol.*, 2001, **62**, 1579–1585.
39 V. Lanza and G. Vecchio, *J. Inorg. Biochem.*, 2009, **103**, 381–388.
40 V. Oliveri, A. Puglisi and G. Vecchio, *Dalton Trans.*, 2011, **40**, 2913–2919.